WAVELENGTH OPTIMIZED ELECTRO-OPTIC SCANNING OF MMICS WITH FABRY-PEROT ENHANCEMENT

P. O. Müller, D. Erasme, and B. Huyart

Communications Department, ENST
46 rue Barrault, Paris cedex 13, France

Abstract— **We present a direct, internal electro-optic probing technique using a CW DFB laser diode. Optical Fabry-Perot resonance offers an immediate AM electro-optic signal. No polarization treatment of the probe beam is needed and a simplified fiber reinjection set-up is realized. During the scanning of MMICs, active wavelength control provides optimum measurement sensitivity.**

Introduction

Different types of electro-optic probing techniques have been developed in the past in order to obtain more detailed information about the electric field distribution inside of complex MMICs (microwave monolithic integrated circuits). Internal and external electro-optic probing systems help improving electric models for semiconductor devices and support the development of new integrated circuits [1], [2]. The linear electro-optic effect gives access to a very fast and non-invasive measurement of electric fields on such devices. However, the usually observed phenomenon is a polarization change of the probing laser beam that has to be transformed into an amplitude modulated (AM) signal. This signal is proportional to the electric field, present on the device, and can be detected by a photodiode. In contrast to the polarization analysis, there have been some reports about the Fabry-Perot enhanced internal probing [3], [4]. This approach reveals some calibration methods and a direct AM component in the electro-optic signal. In our contribution, we present an internal probing technique allowing direct electro-optic AM of the probing light intensity. The probe beam preparation is going to be simplified, and an active wavelength control assures the accurate electro-optic signal during the scanning of an MMIC section.

Experiment

With intent to reduce experimental set-up dimensions, a semiconductor laser diode and fibred optical components are used. The set-up is described in Fig. 1. A distributed feedback (DFB) multiquantum-well laser diode at $1550\,nm$ provides a $1\,mW$ continuous wave (CW) probe beam. The laser is temperature controlled in order to stabilize power and wavelength. The optical circulator separates the probe beam from the reflected electro-optical modulated signal beam. Since we confine a

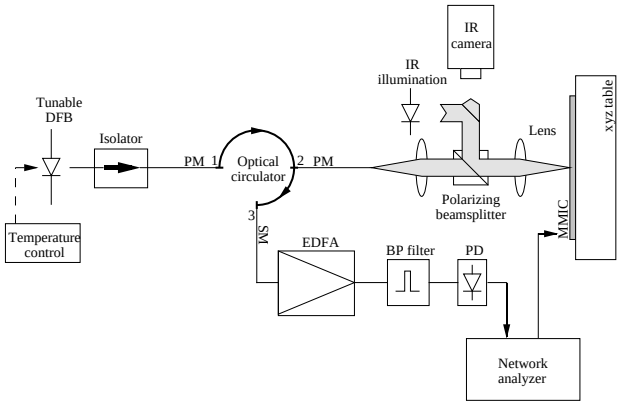

Fig. 1. Experimental Set-up

linearly polarized probe beam to one principal axis of the GaAs substrate, polarization maintaining (PM) fibers can be used at the circulator connections 1 and 2. A confocal arrangement of the fiber 2 end and the backside

0-7803-4603-6/97/$5.00 (c) IEEE

metallization of the device under test leads to a high quality reinjection of the electro-optic signal into the same fiber. The observation system operates through the polarizing beamsplitter and uses also infrared illumination light to avoid eventual perturbation of the device function. On the other hand, the beamsplitter has no impact on the probe signal. The electro-optical modulated light is guided by the circulator to fiber 3 and amplified by an erbium doped fiber amplifier (EDFA). Before detecting the AM signal, a $1\,nm$ bandpass filter eliminates a large part of the high spontaneous emission produced by the EDFA, thus reducing the noise level on the fast photodiode (PD). The bandwidth of this photodiode is the limiting factor in regard to the time resolution of the set-up. The network analyzer generates and detects the electric signal. In order to scan precise MMIC sections, an xyz-table is moved by micrometer step-motors.

Along with the CW internal electro-optic probing configuration, Fabry-Perot resonance inside the substrate is present. It depends on the choice of the numerical aperture (NA) of the focusing lens, whether this resonance is observable or not. Since we do frontside injection probing on microstrip line circuits, this choice is limited by the maximum spatial resolution we are to obtain. For a gaussian beam model, assuming a wavelength around $1550\,nm$ and a substrate thickness of $100\,\mu m$, this spatial resolution approaches $10\,\mu m$ using an optimal NA of 0.25. We described in an earlier publication the behavior of a Fabry-Perot enhanced electro-optic signal [4]. In this new experimental set-up, the probe beam is linearly polarized parallel to one principal axis of the crystal index ellipsoid. No birefringence has to be considered. Thus, based on the Airy equation (1) for reflected light by two parallel planes, we develop new terms in order to describe the reflected average light intensity I_{avg} and its electro-optic AM excursion I_{eo}. This last expression represents the direct electro-optic AM of the probe beam without any further polarizer interaction. Φ is the electro-optic phase modulation within the substrate.

$$E_{ref} = -E_i \left(\frac{r + Re^{-j\phi}}{1 + rRe^{-j\phi}} \right) \tag{1}$$

$$I_{avg} = I_0 \frac{r^2 + R^2 + 2rRcos(\frac{4\pi n_0 h}{\lambda})}{1 + r^2R^2 + 2rRcos(\frac{4\pi n_0 h}{\lambda})} \tag{2}$$

$$I_{eo} = I_0 \Phi \frac{4rR(1-r^2)(1-R^2)|sin(\frac{4\pi n_0 h}{\lambda})|}{(1 + r^2R^2 + 2rRcos(\frac{4\pi n_0 h}{\lambda}))^2} \tag{3}$$

$$\Phi = \frac{2\pi}{\lambda} n_0^3 r_{41} \int_0^h E_z dz \tag{4}$$

where E_i is the field amplitude of the injected probe beam, I_0 its intensity, r and R are the front- and backside reflection factors, n_0 and h the refractive index and the thickness of the substrate, λ is the wavelength of the probe beam, r_{41} the linear electro-optic coefficient and E_z the amplitude of the applied electric signal, z being the longitudinal principal axis in the direction of the probe beam. Internal losses are contained in the reflection factors.

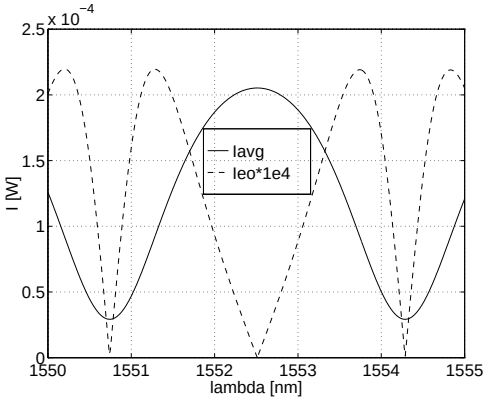

Fig. 2. Resonance Curves of I_{avg} and I_{eo}

Fig. 2 represents the theoretical behavior of the average intensity and the electro-optic signal. ($I_0 = 0.75mW$, $r = 0.55$, $R = 0.32$, $n_0 = 3.4$, $h = 100\,\mu m$, $V_{pp} = 1V$). V_{pp} accounts for the electric field integral over z. The two equations show a derivative relation. For

the following discussion of the results we may keep in mind, that the optimum electro-optic signal is not detected at the maximum average intensity.

Results

The theoretical description of the Fabry-Perot resonance shows, that a correct and optimum electro-optic signal detection can only be achieved by wavelength control. A combined temperature and bias current control on the DFB laser fixes the optimum wavelength at each measurement point. The two measured signals in Fig. 3 show a typical resonance response of a $100\,\mu m$ GaAs substrate. In the given example the optimum wavelength has to be taken at $1553.2\,nm$ and the final electro-optic signal normalized by the corresponding laser intensity. In order to verify the accuracy of the wavelength control, we first do a standard measurement of the potential next to a $10\,\mu m$ microstrip line. Fig. 4 shows the exponential decrease of the potential amplitude with increasing distance. The first three measurement points are taken on the metallization of the line. We find a minimum detectable signal level of $-35\,dBm$ at $1\,Hz$ resolution bandwidth.

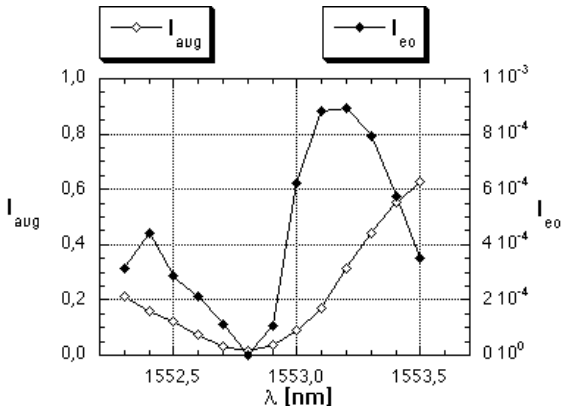

Fig. 3. Resonance of the Electro-optic Signal

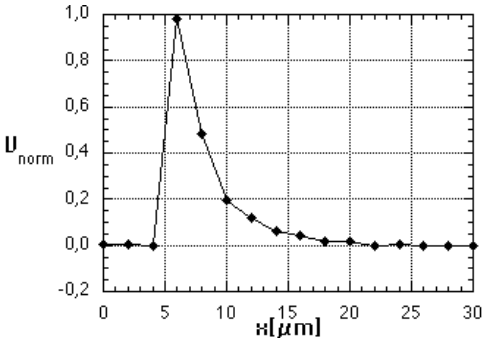

Fig. 4. Potential decrease

Finally we do a 2-D scan of a MMIC section. Fig. 5 shows the layout of an inductor connection to a $50\,\Omega$ microstrip line. This MMIC has a substrate thickness of $100\,\mu m$ and the line width is $10\,\mu m$. The optimum spatial resolution of the frontside internal probing is attained resolving the present structure. We have measured a $2\,GHz$ electric signal in this section, on the one hand using the active wavelength control during the scan (Fig. 6), on the other hand optimizing the wavelength at one position and doing the whole scan with this same wavelength (Fig. 7). The two figures present the normalized potential distribution. It turns out, that the active wavelength control is able to compensate FP resonance perturbations as they can be recognized in the upper right part of Fig. 7. Furthermore, the potential variations along the microstrip line are also indicator of the signal deterioration with displacement over the section. However, one can see slight signal deformation also in Fig. 6, almost opposite to the T-connection point. This remaining deterioration is due to stronger changes of the reflection factors r and R. In order to calibrate their influence on the electro-optic signal, the resonance curve of the average light reflection needs to be caracterized at each scan position.

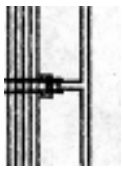
Fig. 5. T-structure on MMIC

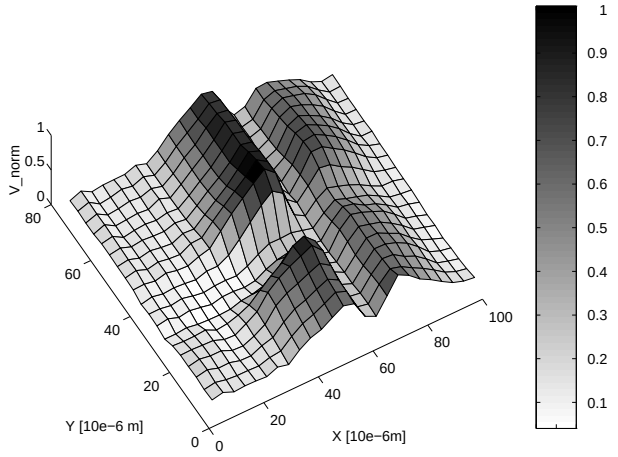

Fig. 6. Potential with Wavelength Control

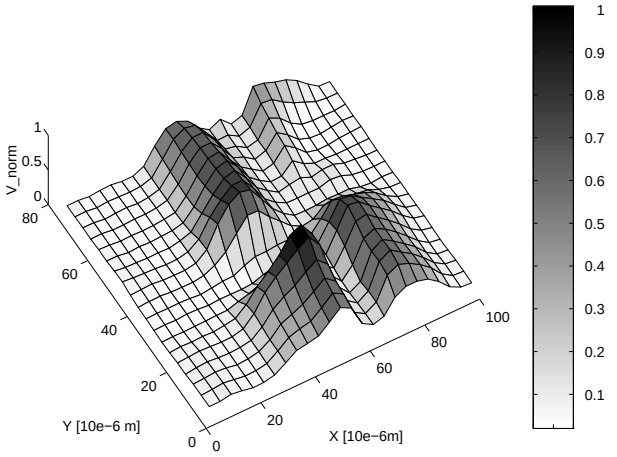

Fig. 7. Potential without Wavelength Control

Conclusions

In internal electro-optic probing the Fabry-Perot resonance is present and can provide an immediate AM signal. Therefore, a simplified system configuration with a semiconductor laser source and fibred optical components has been presented. The signal improvement by the active wavelength control has been demonstrated doing a 2-D MMIC scan. However, in order to obtain absolute electric field data respecting the change of the reflection factors, the behavior of the average light resonance curve needs to be characterized. Finally, the FP resonance is limited by the NA of the focusing lens.

References

[1] Yutaka Imaizumi, Mitsuru Shinagawa, and Hiroyo Ogawa, "Electric Field Distribution Measurement of Microstrip Antennas and Arrays Using Electro-Optic Sampling," IEEE Trans. Microwave Theory Techn., vol. 43, no. 9, pp. 2402-2407, 1995

[2] G. David, P. Bussek, U. Auer, F. J. Tegude, and D. Jäger, "Electro-optic probing of RF signals in submicrometre MMIC devices," Electronics Letters, vol. 31, no. 25, pp. 2188-2189, 1995

[3] D. R. Hjelme, A. R. Mickelson, "Voltage Calibration of the Direct Electrooptic Sampling Technique," IEEE Trans. Microwave Theory Techn., vol. 40, no. 10, pp. 1941-1950, 1992

[4] D. Le Quang, D. Erasme, and B. Huyart, "MMIC-Calibrated Probing by CW Electrooptic Modulation," IEEE Trans. Microwave Theory Techn., vol. 43, no. 5, pp. 1031-1036, 1995

0-7803-4603-6/97/$5.00 (c) IEEE